Available online at www.sciencedirect.com
ScienceDirect
Journal of Sound and Vibration 324 (2009) 91–106
JOURNAL OF SOUND AND VIBRATION
www.elsevier.com/locate/jsvi

Investigation of the underlying cause of the interaction between acoustic resonance and fluidelastic instability in normal triangular tube arrays

John Mahon*, Craig Meskell

School of Engineering, Trinity College Dublin, Ireland

Received 29 May 2008; received in revised form 15 January 2009; accepted 22 January 2009
Handling Editor: C.L. Morfey
Available online 19 March 2009

Abstract

The interaction between fluidelastic instability and acoustic resonance in a normal triangular tube array has been previously quantified, although no physical mechanism was identified. In this study interaction between fluidelastic instability and acoustic resonance is extended to a second array. In addition, to assess the interaction between fluidelastic instability and acoustic resonance two possibilities are examined. The first examines the effect of acoustic resonance on the static fluid forces on a stationary cylinder and the second the effect of acoustic resonance on the time delay between tube motion and the resultant flow reorganisation close to the measurement cylinder. It is found that acoustic resonance did not modify the static fluid force. Acoustic resonance is seen to modify the time delay between tube motion and flow field around the cylinder. It is proposed that acoustic streaming is affecting the time delay process resulting in the drop in fluidelastic vibration amplitude observed.

1. Introduction

It is well known that an array of circular tubes subject to fluid cross-flow may exhibit large amplitude self-induced vibration known as fluidelastic instability (FEI). Chen [1] classified the phenomenon under two distinct mechanisms: fluid damping controlled instability and fluid stiffness controlled instability. This study is concerned with fluid damping controlled instability. Instability occurs in this mechanism when the fluid damping goes negative. Furthermore, it has been suggested that there is a time delay between tube motion and the resulting fluid forces at the root of the damping controlled mechanism.

As the array is enclosed within a duct, the system may also experience acoustic resonance in addition to fluidelastic instability, the frequency of which may be several orders of magnitude greater than the fundamental frequency of the structure. Thus, it might be expected that these two phenomena would be independent. This perspective has been widely accepted in relation to the interaction between fluidelastic

*Corresponding author.
E-mail address: mahonjp@tcd.ie (J. Mahon).

0022-460X/$ - see front matter © 2009 Published by Elsevier Ltd.
doi:10.1016/j.jsv.2009.01.045

Nomenclature

A_M, B_M, c	constants
d	tube diameter
f_n	excitation frequency (Hz)
f_s	sample frequency (Hz)
M	number of harmonics
P/d	pitch ratio
u	local velocity component—in-flow direction
U	free stream flow velocity
U_c	critical flow velocity
U_g	gap flow velocity
v	local velocity component—cross-flow direction
v_M	velocity at Mth harmonic
V_r	reduced gap velocity
y	tube displacement
$\dot{y}$	tube velocity
$\ddot{y}$	tube acceleration
$\Delta\phi$	phase difference
Δt	time delay
δ	logarithmic decrement
δ_{st}	structural logarithmic decrement
ζ	damping ratio
ρ	density of air
ω	natural frequency (rad s^{-1})
APV	acoustic particle velocity
AR	acoustic resonance
DC	direct current
EMD	electromagnetic damper
EMS	electromagnetic shaker
FEI	fluidelastic instability
SPL	sound pressure level

instability and vortex shedding or acoustic resonance. However, Price and Zahn [2] and Meskell and Fitzpatrick [3] reported an apparent interaction between fluidelastic instability and acoustic resonance. Price and Zahn reported the fluidelastic behaviour of a single flexible tube in a normal triangular tube array ($P/d = 1.375$) in air. The flexible tube was free to oscillate in both the lift and drag directions. They reported an interaction between fluidelastic instability (~7 Hz) and acoustic resonance (733 Hz). When the flexible tube was mounted in the first row, fluidelastic instability was apparently triggered by acoustic resonance. The acoustic resonance was noted to have organised the flow throughout the tube array. The authors also note that acoustic resonance sometimes had a minor effect on the cylinder vibration amplitude. When the flexible tube was positioned in rows 2–7, there was typically a change in the vibration amplitude coincident with the acoustic resonance. More recently, Meskell and Fitzpatrick reported on the fluidelastic behaviour of a centrally located tube with a natural frequency of 6.6 Hz in a normal triangular tube array with pitch ratio of 1.32. The flexible tube was free to oscillate in the lift direction only. They reported that fluidelastic instability was suppressed when the free stream flow velocity reached 9 m s^{-1}. This was accompanied by an acoustic resonance at 1050 Hz corresponding to the second transverse mode of the duct.

In a previous study the authors [4] reproduced and quantified the apparent interaction between fluidelastic instability and acoustic resonance (second transverse acoustic mode) for a single flexible in a five row normal triangular tube array ($P/d = 1.32$). The approach taken was to artificially excite acoustic resonance and quantify the effect of acoustic resonance on fluidelastic instability by modifying three independent variables: speaker power (i.e. sound pressure level), free stream flow velocity and structural damping. The current study briefly recalls the quantification of the effect of acoustic resonance on fluidelastic instability for $P/d = 1.32$ extending the analysis to include $P/d = 1.58$ before proceeding on to a more comprehensive analysis of the interaction between the phenomena.

2. Experimental setup

Tests were carried out in draw down wind tunnel with a velocity range from 2 to 14 m s^{-1} with a free stream turbulence intensity of less than 1%. The flow velocity was measured using a pitôt-static tube coupled with a micromanometer installed upstream of the test section. An array of 38 mm cylinders in a normal triangular configuration was housed in the test section as shown in Fig. 1. The arrays under test were two five row normal triangular tube arrays with pitch ratios of 1.32 and 1.58. The tubes in the array are rigidly fixed, except for one tube which will be referred to as the instrumented cylinder (shaded cylinder, Fig. 1). For vibration tests, the

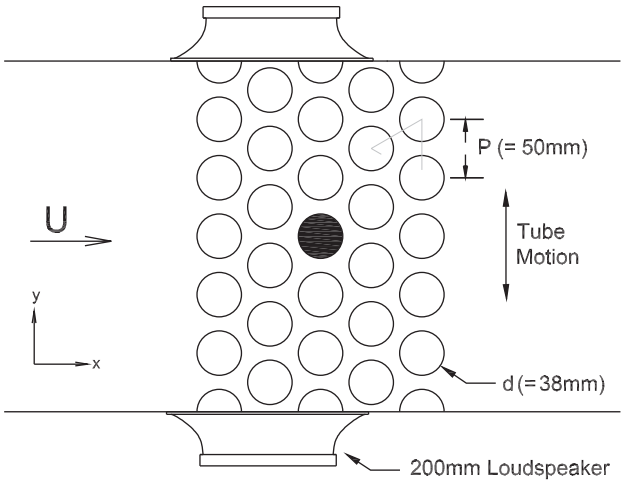

Fig. 1. $P/d = 1.32$; test section schematic.

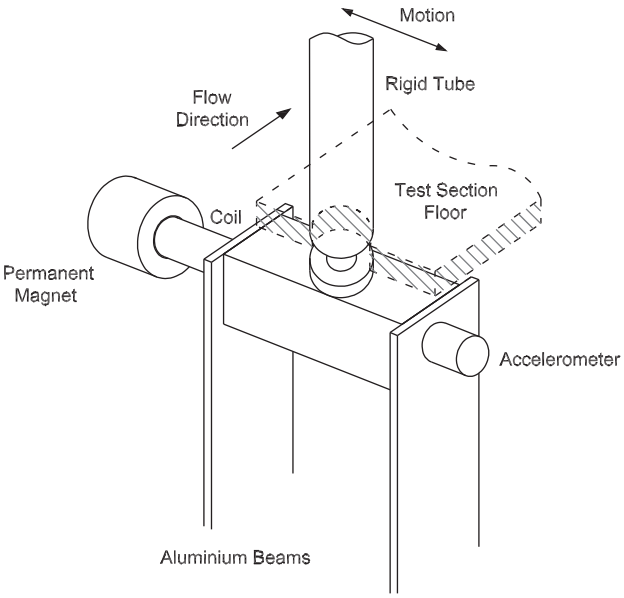

Fig. 2. Flexible tube with the electromagnetic damper in situ.

instrumented cylinder was flexibly mounted and was free to oscillate in the lift direction, y, only. The tube is rigid in construction, however, it is mounted on a flexible cantilevered support outside of the tunnel which is isolated from the wind tunnel test section. The structural damping of the system is controlled by a simple non-contact electromagnetic damper (EMD) consisting of a permanent magnet, a coil and a range of variable resistors. The level of damping is set by modifying the resistance in the circuit. The advantage of this setup is that there is no mechanical connection between the magnet and the coil so there is no change in structural stiffness [3]. A schematic illustrating the mounting scheme for the flexible tube as well as the electromagnetic damper can be seen in Fig. 2. Also shown is a sectioned view of the test section floor through which the flexible tube was situated. The electromagnetic damper /shaker arrangement was also used for forced vibration tests by applying a voltage across the coil. For the force measurement tests, the instrumented tube had 36 surface pressure taps at 10° intervals located along the centre span of the tube which was mounted on an $x-y$ traverse (located outside the wind tunnel). Each tapping was monitored with a dedicated pressure transducer.

Artificial excitation of acoustic resonance in the tube array was performed using two 225 W speakers (Eminence Beta 8) located on both side walls of the test section as shown in Fig. 1. The speakers were wired in anti-phase and driven by a HP35665A dynamic signal analyzer via USA 370 amplifier to excite the second acoustic mode of the duct.

The tube oscillation was measured using a PCB quartz shear accelerometer with a useful range of 0.2–7000 Hz (based on a maximum 5% variation in sensitivity). The accelerometer was mounted on the tube support as shown in Fig. 2. The acoustic sound pressure level was measured using 6.7 mm (G.R.A.S) microphones flush mounted in the test section. The microphones had a sound pressure level upper limit of 194 dB with 3% distortion. A Brüel and Kjaer Sound Level Calibrator Type 4231 was used to calculate the sensitivity of the microphones at a frequency of 1000 Hz and a pressure of 1 Pa (94 dB). Surface pressure was measured using Senotec 24 PC Series differential pressure transducers with the reference vented to atmosphere. In effect the gauge pressure was measured. Local flow velocity measurements were made using a single hot-wire probe which was rotated to measure both the u and v direction velocity components. The hot-wire anemometer used in this setup was a DISA 55M01 system with a 55M10 Constant-Temperature Anemometer standard bridge. The readings from these instruments were digitised and logged using an National Instruments 8 channel (NI PXI-4472B), 24 bit data acquisition frame. Each channel was simultaneously sampled and automatically low pass filtered to avoid aliasing. Additional information about the test setup and equipment used can be found in Mahon [5].

3. Results

In the first instance, it was verified that a single flexible cylinder in the pitch ratios of 1.32 and 1.58 became unstable due to fluidelastic instability. At each flow velocity the tube was given time to establish a steady motion. Tube acceleration was then measured for 600 s at a sample frequency of 64 Hz to acquire a steady RMS value of vibration amplitude. With anti-aliasing filters the dynamic range was 0–29 Hz. Within this frequency range only the first structural mode (6.6 Hz or 41.47 rad s^{-1}) was measured with the higher frequency modes not included. From the tube acceleration data, an estimate of the tube displacement was extracted. As the flow velocity was increased, fluidelastic instability was apparent and was characterised by the rapid increase in vibration amplitude. The change in slope of the vibration amplitude curve has been used as a practical definition of threshold velocity, U_c (e.g. Ref. [6]). The alternative definition of critical velocity based on amplitude levels (rather than amplitude gradients) proposed by Yeung and Weaver [7] was also satisfied. Fig. 3 plots the stability threshold in terms of reduced gap velocity and mass damping parameter together with data from Austermann and Popp [6] and Price and Zahn [2]. These two sources were chosen as they have a

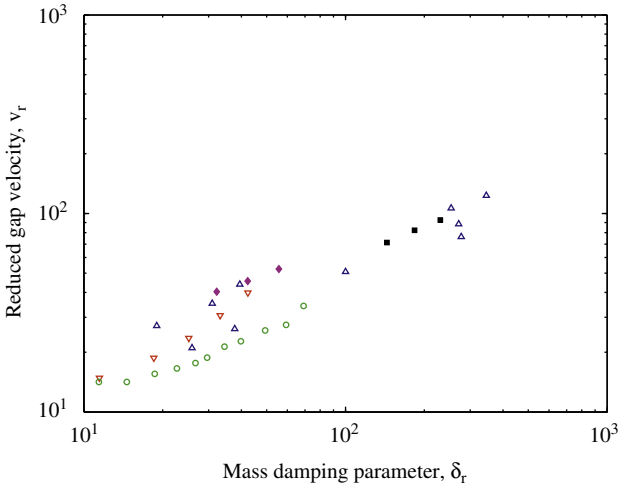

Fig. 3. Comparison of measured stability thresholds: ○, Austermann and Popp [6], $P/d = 1.25$; ▽, Austermann and Popp [6], $P/d = 1.375$; △, Price and Zahn [2], $P/d = 1.375$; ■, present, $P/d = 1.32$; ◆, present, $P/d = 1.58$.

similar set up to the current experiments (a single flexible cylinder in a normal triangular array and air as the working fluid). It can be seen that the current results compare favourably with the data available.

3.1. Effect of acoustic resonance

3.1.1. Pitch ratio = 1.32

The effect of acoustic resonance on fluidelastic instability was quantified for the pitch ratio of 1.32 in a previous paper [4]. A brief review of the measurements and results are presented here. The effect of acoustic resonance on fluidelastic instability was quantified by artificially exciting the duct acoustics at various loudness levels and for a range of flow velocities and levels of structural damping. Acoustic resonance was found to modify the fluidelastic vibration amplitude. Fig. 4 shows a time trace of tube displacement at $\delta_{st} = 0.088$ and $U = 4.5\,\mathrm{m\,s^{-1}}$ with and without acoustic excitation. At $t = 0\,\mathrm{s}$ acoustic excitation was applied with a speaker power of 64 W (SPL = 140 dB). It was seen that the effect of acoustic resonance was to reduce the vibration amplitude by more than 50%. In fact, the applied acoustic field increased the critical velocity, delaying the onset of fluidelastic instability as illustrated in Fig. 5.

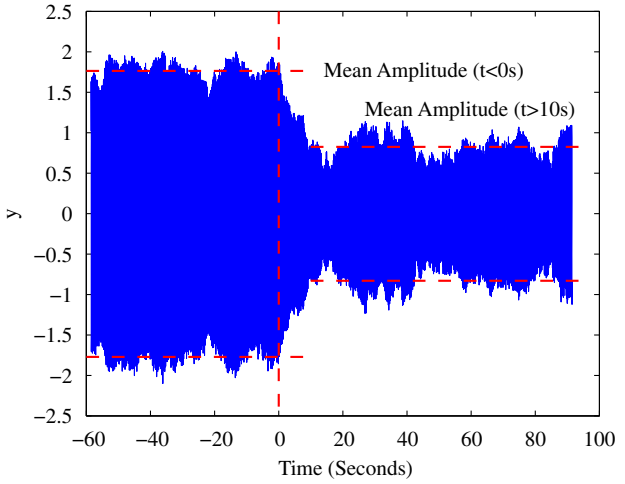

Fig. 4. $P/d = 1.32$; time trace of tube displacement. Acoustic excitation applied at $t = 0\,\mathrm{s}$.

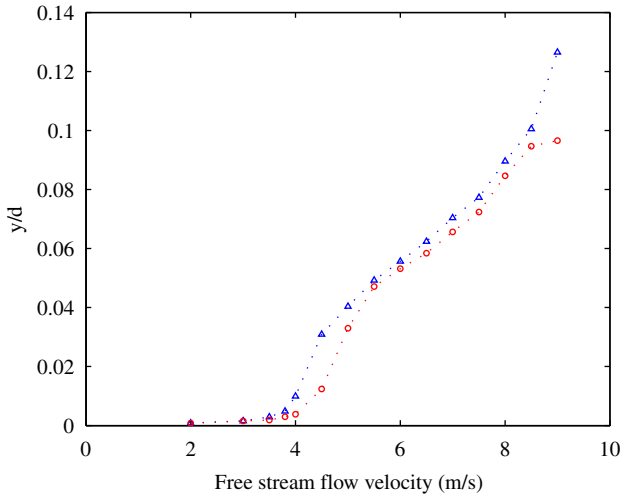

Fig. 5. RMS of tube vibration at $\delta_{st} = 0.088$: △, without acoustic excitation and ○, with artificially excited acoustic resonance (speaker power = 32 W).

It was also shown that the effect of acoustic resonance on fluidelastic instability was dependent on speaker power. The fluidelastic vibration amplitude reduces with increasing speaker power as illustrated in Fig. 6. It was also apparent that the effect of acoustic resonance on fluidelastic instability was dependent on flow velocity and structural damping. The effect of the acoustic resonance on fluidelastic vibration amplitude varied with cross-flow velocity but the nature of this was uncertain. Also, the lower the structural damping, the more responsive the fluidelastic mechanism was to the artificially excited acoustic resonance. In terms of the system dynamics, acoustic resonance adds damping reducing the apparent negative fluid damping associated with fluidelastic instability. Further results on the interaction between acoustic resonance and fluidelastic instability for $P/d = 1.32$, as well as the identification technique for obtaining the fluid damping can be found in Mahon and Meskell [4].

3.1.2. *Pitch ratio* = 1.58

Experimental results on the effect of acoustic resonance (1106 Hz) on fluidelastic instability in the pitch ratio of 1.58 which have not been published previously are examined in this section. Fig. 7 shows a sequence of tests

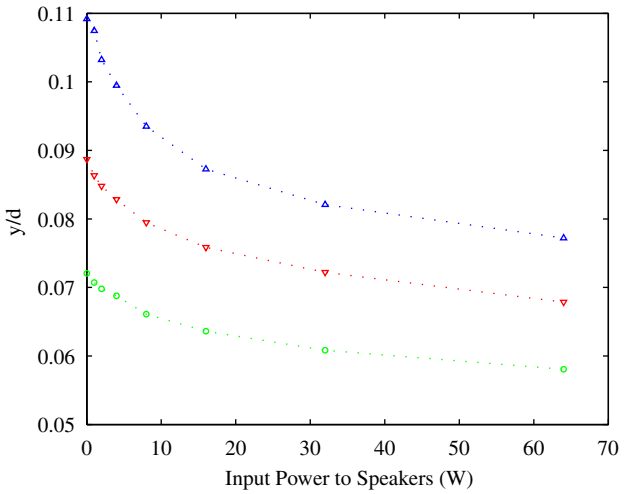

Fig. 6. $P/d = 1.32$; vibration amplitude against input power to speaker: △, $\delta_{st} = 0.077$; ▽, $\delta_{st} = 0.098$; ○, $\delta_{st} = 0.123$.

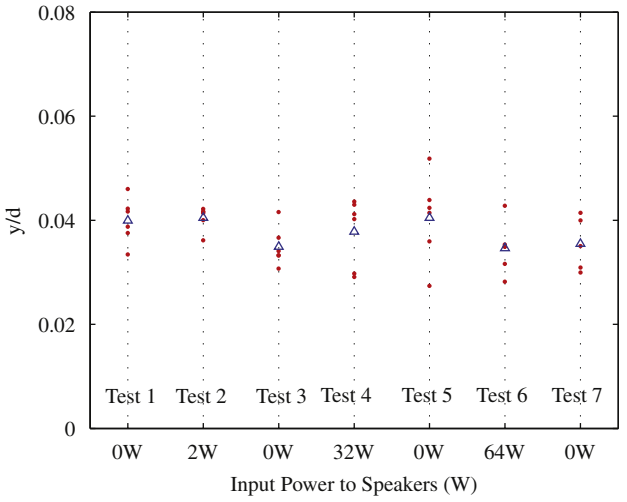

Fig. 7. $P/d = 1.58$; sequence of tests from left to right showing vibration amplitude against speaker power at $U = 9\,\mathrm{m\,s^{-1}}$ and $\delta_{st} = 0.030$. •, individual test; △, average of the five tests.

conducted at a structural damping level (δ_{st}) of 0.030 and a flow velocity (U) of $9\,m\,s^{-1}$. The test sequence (1–7) moves from left to right with the input power to the speaker varying accordingly (l to r: 0, 2, 0, 32, 0, 64, 0 W). The tests were repeated five times. It was observed that the acoustic resonance had no significant effect on the vibration amplitude. The amplitude varied from test to test independently of whether forced acoustics was applied or not. It was also observed the amount of scatter varies from test to test. For example, there is significantly less scatter in test 2 compared with test 5. This is due to the jet switching phenomenon observed in this pitch ratio. Fig. 8 shows the time resolved pressure signal from a pressure tapping ($\theta = 230^\circ$ see Fig. 13 for angular positioning) on a static cylinder at the same location as the flexible tube. There appears to be a bi-stable flow regime (jet switching) in the pitch ratio of 1.58. Fig. 9 examines the limit cycle amplitude of the flexible tube when the system was in a post stable regime. It was found that well established limit cycle amplitudes are observed for the pitch ratio of 1.32 but not for $P/d = 1.58$; the response was dominated by the natural frequency, but the response was more akin to forcing by a narrow band random excitation which could be explained by the jet switching observed. It is also clear from the viewing of both Figs. 8 and 9 that the phenomena of jet switching is sporadic in nature and hence, this is why such a difference in scatter was observed from test to test. Further details on jet switching and surface pressure measurements in tube arrays can be found in Mahon [5].

Tests examining the effect of acoustic resonance on fluidelastic instability for the pitch ratio of 1.58 were repeated for other flow velocities and levels of damping. More specifically, for a structural damping level of 0.030, tests were also conducted at a velocity of $11\,m\,s^{-1}$ and for a structural damping level of 0.017, tests were conducted for velocities of 7 and $9\,m\,s^{-1}$. Irrespective ofwhich data set was examined the outcome remained the same, that is the effect of acoustic resonance on fluidelastic instability in the pitch ratio of 1.58 was negligible.

It was found that acoustic resonance was shown to affect the fluidelastic behaviour of a single flexible cylinder in the pitch ratio of 1.32, however, no effect was found for the pitch ratio of 1.58. This suggests a fundamental difference in the fluidelastic behaviour between the two arrays tested and is discussed below.

3.2. Possible physical mechanisms

The effect of acoustic resonance on fluidelastic instability has been quantified above. However, it is difficult to envisage the physics of a true interaction between fluidelastic instability and acoustic resonance. In a previous study the authors [4] examined alternatives to an interaction between the two phenomena which could explain the observations discussed.

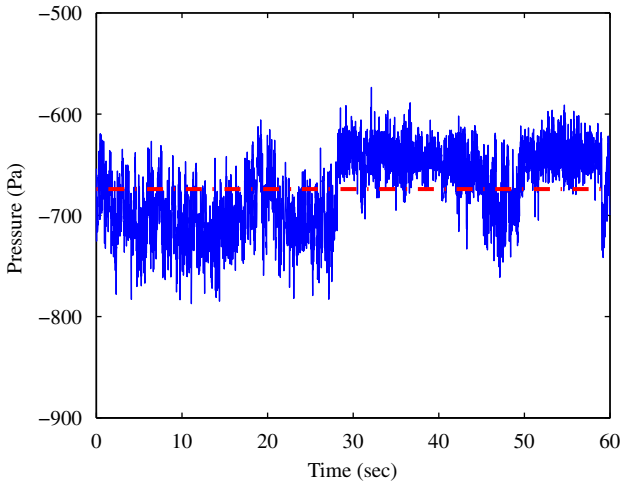

Fig. 8. Time resolved pressure signal; $y/d = 0\%$ at $\theta = 230^\circ$.

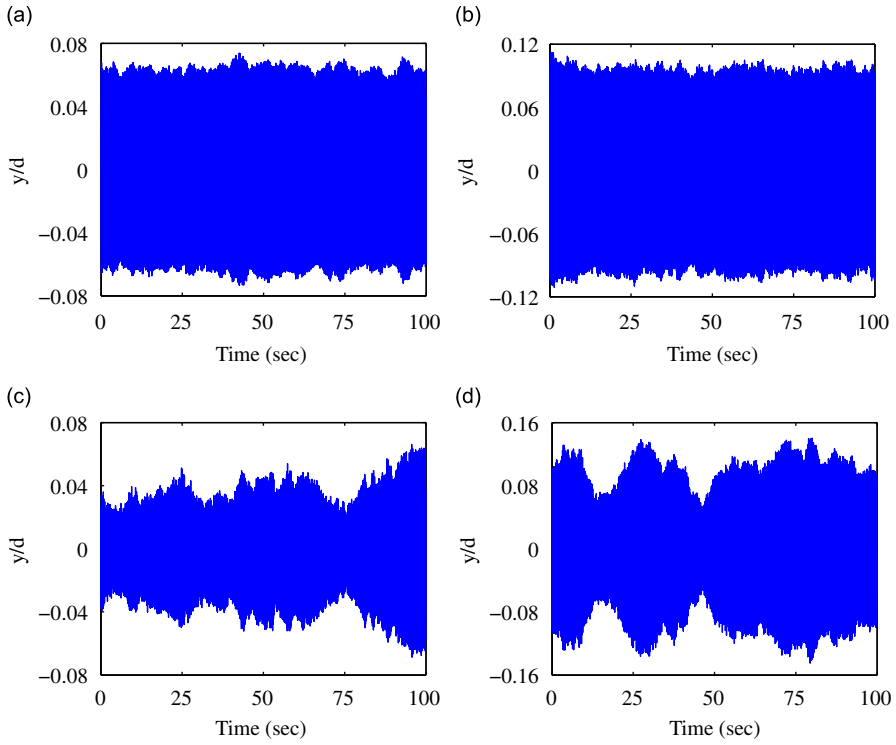

Fig. 9. Tube motion when the tube is vibrating in a post stable regime for $P/d = 1.32$ and 1.58 at various flow velocities: (a) $P/d = 1.32$; $\delta_{st} = 0.123$, $U = 4.5\,\mathrm{m/s}$; (b) $P/d = 1.32$; $\delta_{st} = 0.123$, $U = 6.5\,\mathrm{m/s}$; (c) $P/d = 1.58$; $\delta_{st} = 0.030$, $U = 9\,\mathrm{m/s}$; (d) $P/d = 1.58$; $\delta_{st} = 0.030$, $U = 13\,\mathrm{m/s}$.

- It was reported that acoustic resonance adds positive damping. Tests in quiescent fluid showed that the sound field did not provide an additional damping force independently of the flow, meaning superposition of independent phenomena was excluded.
- Blevins and Bressler [8] and Feenstra et al. [9] reported that acoustic resonance can cause a change in the pressure drop across the array, hence a change in the free stream flow velocity. Such findings were not observed.
- Relocating the flexible cylinder to examine the effect of acoustic particle velocity (APV) did not result in a significant change in behaviour, indicating that the effect of acoustic particle velocity was small.

4. Interaction between fluidelastic instability and acoustic resonance explored

It was reported above that acoustic resonance was found not to have an effect on fluidelastic vibration amplitude in $P/d = 1.58$, so the analysis in this section is restricted to $P/d = 1.32$. However, an explanation as to why acoustic resonance had no effect on fluidelastic vibration amplitude for $P/d = 1.58$ in the context of the analysis in this section will be discussed. Two possibilities are examined which are based on the quasi-steady framework proposed by Price and Paidoussis [10] to model fluidelastic instability. Although the analysis was quasi-steady, the resulting fluid damping and stiffness matrices contain frequency dependent terms resulting from the introduction of a time delay effect. In simple terms this separates the fluidelastic force into a magnitude dependent on the static fluid force and a phase dependent on the time delay. In the magnitude dependent part, the fluid forces (lift and drag) are assumed to be identical to those measured with the tube at rest in the same location (this is the quasi-static assumption) and is shown in Eq. (1). The phase dependent (time delay) part is based on the work of Simpson and Fowler [11]. It is argued that the origin of the time delay was twofold: there is a time delay between the fluid particles leaving an upstream row of cylinders

and arriving at a downstream row cylinders; and, a flow retardation effect as the flow approaches the cylinder. Because the flow slows down as it approaches the cylinder, the resulting fluid flow arrives at the cylinder at some interval of time later than it would have done had the flow velocity been constant. Irrespective of the origin of the time delay, Price and Paidoussis assuming harmonic motions introduces the time delay into Eq. (1) yielding Eq. (2). This can be further manipulated to calculate the critical velocity for the onset of fluidelastic instability . Granger and Paidoussis extended the model to use a memory function due to vorticity convection but for sinusoidal motion, this will reduce to a time delay

$$F_y = \frac{1}{2}U^2 ld\left[\left(\frac{\partial C_L}{\partial y}\right)y - C_{D_0}\left(\frac{\dot{y}}{U}\right)\right] \tag{1}$$

where $\partial C_L/\partial y$ is the change in lift force with tube displacement, C_{D_0} is the drag force at zero displacement

$$F_y = \frac{1}{2}U^2 ld\left[\mathrm{e}^{-i\omega\Delta t}\left(\frac{\partial C_L}{\partial y}\right)y - C_{D_0}\left(\frac{\dot{y}}{U}\right)\right] \tag{2}$$

It is seen in Eq. (2) that the fluid force separates into two components: the static fluid forces (steady effects) $\partial C_L/\partial y$ and C_{D_0}; and unsteady effects caused by the time delay Δt.

4.1. Effect of acoustic resonance on the static fluid force

The effect of acoustic resonance on the surface pressure distribution around a static cylinder in the third row of the array was examined. Tests were conducted for a number of flow velocities ($U = 2, 4, 6, 7, 8, 10\,\mathrm{m\,s^{-1}}$); and at a range of tube displacements ($y/d = 0\%$, 1%, 3%, 5%, 7%, 10%); at various speaker input power (0, 16, 32, 64 W). The mean pressure was measured for 120 s at sample rate of 64 Hz. The pressure data were integrated into fluid forces (lift and drag).

Figs. 10 and 11 show the mean pressure distribution with and without forced acoustics at the second acoustic mode of the duct. At the lower velocities of 2 and $4\,\mathrm{m\,s^{-1}}$, acoustic resonance has a small effect on the mean pressure distribution. The effect of the imposed acoustics shows a lesser effect at the higher velocities of 6, 7, 8 and $10\,\mathrm{m\,s^{-1}}$. When the tube was displaced similar findings were observed. The small changes in pressure distribution at lower velocities were not translated into any significant effect on the lift and drag. Fig. 12 plots the lift and drag coefficient at $y/d = 5\%$ without forced acoustics (0 W) and with forced acoustics at three levels; 16, 32 and 64 W. Differences between the data with and without forced acoustics are observed. However, no trend emerges as a function of speaker power (or sound pressure level). Furthermore, the differences observed between the data sets are comparable to the random variation in the data. Thus, the effect

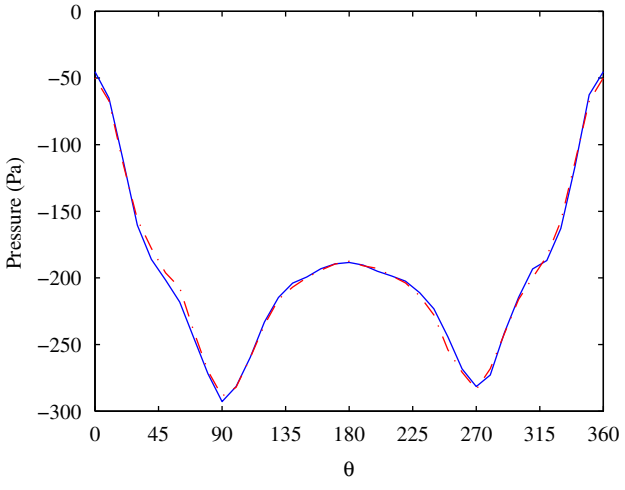

Fig. 10. Pressure distribution around at $U = 4\,\mathrm{m\,s^{-1}}$: –, no acoustics; – · –, frequency = 1092 Hz (SPL = 140 dB).

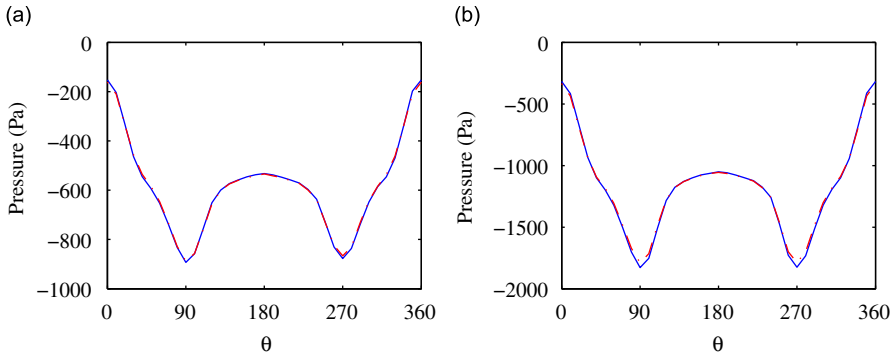

Fig. 11. Pressure distribution around at (a) $U = 7\,\mathrm{m\,s^{-1}}$ and (b) $U = 10\,\mathrm{m\,s^{-1}}$: –, no acoustics; – · –, frequency = 1092 Hz (SPL = 140 dB).

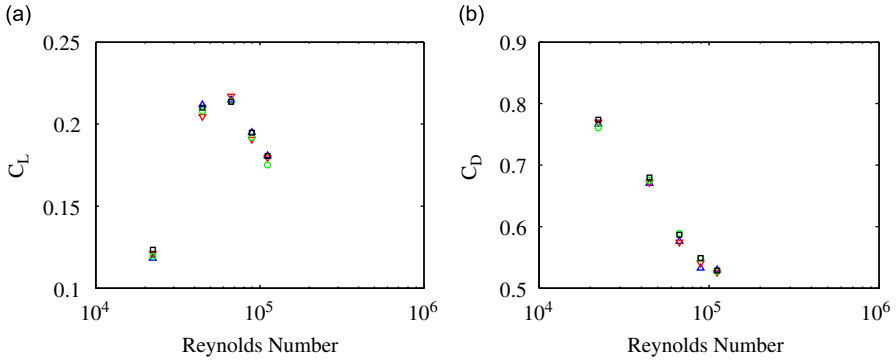

Fig. 12. Lift and drag coefficient against Reynolds number, with and without imposed acoustics. △, 0 W; ▽, 16 W; ○, 32 W; □, 64 W.

of the second acoustic mode on the cylinder was minimal, suggesting that acoustic resonance was not affecting the static forces on the cylinder surface. A maximum sound pressure level of 140 dB was used which corresponds to a pressure of 200 Pa. It is acknowledged that at higher sound pressure levels that the effect of acoustic resonance on the mean surface pressure would be more significant as reported by Fitzpatrick et al. [12]. They reported that artificially excited acoustic resonance (160 dB) modified the pressure distribution around cylinders in the 13th row of a 26 row in-line array ($P/d = 1.73$). Acoustic resonance altered the velocity gradients across the array thus modifying the force on the cylinder. In the current study, where the sound pressure level was an order of magnitude lower, the effect on the static fluid force was small. Hence, it is concluded that the modification of static fluid forces is not the cause of the observed interaction between fluidelastic instability and acoustic resonance.

4.2. Time delay

When fluidelastic instability is discussed in the literature, a time delay between the tube motion and the resulting fluid forces is thought to be at the root of fluidelastic instability . The exact nature of the time delay is unclear and has yet to be measured directly. There is some evidence that it exists; Granger and Paidoussis [13] indirectly measured the cause of the time delay using experimental data and a quasi-unsteady model. Abd-Rabbo and Weaver [14] conducted a flow visualisation on rotated square array with $P/d = 1.41$ and water cross-flow. For a single flexible cylinder, flow visualisation ‘‘revealed clear flow redistribution with a phase lag’’. Numerous studies have measured fluid stiffness and damping from which the time delay could be

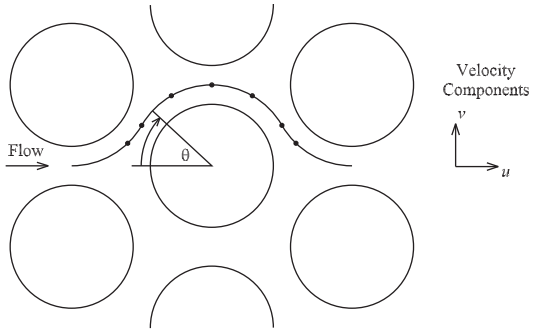

Fig. 13. Hot-wire positions around the instrumented cylinder.

inferred e.g. Refs. [15,16]. It is also apparent that the inclusion of a time delay or phase lag is a prerequisite for the models developed, as without a time delay, the phenomenon cannot be modelled. However, the uncertainty about the origin of the time delay results in different physical explanations for the inclusion of a time delay in the models to predict fluidelastic instability . Nonetheless, Andjelic and Popp [17] showed the importance of a time delay, comparing their experimental data with the "wavy wall channel model" developed by Lever and Weaver [18]. The time delay in the Lever and Weaver model was obtained from various geometric length scales. Andjelic and Popp found that the fit between the analytical curve and experimental data was poor. Modifying the geometric length scales changed the time delay and the stability boundary. A modification in the time delay of the other models will also result in a change in the stability boundary. Indeed, the parameter values for the memory function of Granger and Paidoussis are obtained by fitting the model to experimental threshold data.

An attempt to measure a time delay between tube motion and a point in the flow located near the flexible cylinder is discussed. In an ideal setup, a time delay between tube motion and fluid forces would be measured. This was not achievable due to limitations in the setup. The justification for the current approach stems from the fact that the fluid forces on the cylinder are as a direct consequence of what is happening in the flow around the cylinder. Hence a relationship between the fluid flow and fluid forces are closely related. It therefore seems reasonable to measure the response of the fluid instead of the fluid force as a first attempt to measure the time delay. This conceptual approach is also consistent with the assumption of the Lever and Weaver [18] model.

The flexible cylinder was forced to vibrate at its natural frequency of 6.6 Hz. This was achieved using the electromagnetic shaker (EMS) system described previously. The input signal was generated using a HP35665A dynamic signal analyzer via a USA 370 amplifier. The excited vibration amplitude chosen corresponded to 2.5% tube diameter (an RMS value of 1.8%). Using the electromagnetic damper the maximum level of damping achieved was $\delta_{st} = 0.205$. In an effort to reduce the effect of turbulent buffeting additional damping was added. This was achieved by adhering lengths of rubber to the cantilever support. This modification resulted in the damping increasing from $\delta_{st} = 0.205$ to 0.410. At the new level of damping the tube did not go unstable due to fluidelastic instability for the velocity range of the wind tunnel. Tests were conducted for three free stream flow velocities: 4, 7 and 10 m s^{-1}. The local velocity around the cylinder was measured using a single hot-wire probe located on a curve that was equidistant between the instrumented cylinder and neighbouring cylinders at $\theta = 15^\circ, 30^\circ, 60^\circ, 90^\circ, 120^\circ, 150^\circ$ and 165° (see Fig. 13). Measurements were made in both the in-flow (u) and cross-flow (v) directions. Each test was conducted for 15 s at a sample rate of 8192 Hz. With the excitation frequency of 6.6 Hz this translates to 99 averages thus improving the signal-to-noise ratio by a factor of 10.

4.2.1. Analysis technique

A number of approaches were explored to extract the time delay between the tube response and the local flow velocity. The first approach used the cross-spectrum between the tube response and the local flow velocity

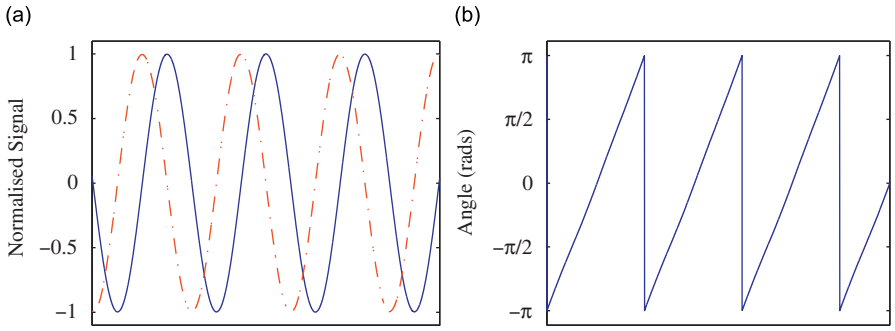

Fig. 14. (a) –, Original signal; – · –, differentiated signal and (b) angular position.

signal to extract the time delay. However, this approach was limited due to the relatively poor frequency resolution that could be resolved given the test parameters. The cross-correlation between the two signals was also attempted, providing improved temporal resolution. However, due to the high level of the random component due to turbulence, the narrow band process due to vortex shedding and the deterministic element due to the acoustic excitation, it was found that this approach did not yield satisfactory results. These problems could conceivably be overcome using a much longer record length, but this is impractical.

As an alternative, the data which are dominated by low frequency components are modelled as a short series of sinusoids in the time domain. This offers the benefits of Fourier analysis (i.e. averaging) with the high temporal resolution achievable with a cross-correlation. For each test, tube motion, local flow velocity and the output signal from the amplifier (input signal to EMS) was acquired. The signal from the amplifier was used as a reference in the analysis as it produced a clean sinusoid whereas the flow velocity and tube response measurements include a random component as both were subject to turbulence in the flow. Note, the level of turbulence in a tube array is very high. The reference signal was differentiated using a central difference method

$$g'(x_0) \approx [g(x_0 + h) - g(x_0 - h)]2f_s \tag{3}$$

where f_s is the sample frequency.

The original and differentiated signals were normalised and the inverse tangent taken on the resultant of the former divided by the latter. This process presents the reference signal in the form of an angular position. A snapshot of these signals is shown in Figs. 14(a) and (b). The flow velocity and tube motion can now be related to an angular position. As the tube motion was forced using a sinusoid at the natural frequency of the structure it might be expected that this would also be observed in the flow surrounding the cylinder. It can be seen (Fig. 15(b)) that this is the case. It is also shown that there is significant scatter in the data. Fitting a harmonic curve to the data removes features from the flow field. However, the phenomenon of concern in the analysis is fluidelastic instability which is dominated by a low frequency sinusoidal response. It is understood that other flow features such as turbulence and vortex shedding exist but are not of concern in this analysis. From the viewing of both the time resolve pressure and velocity measurements in the array jet switching was not observed in this case ($P/d = 1.32$). As fluidelastic instability was phenomenon of interest in this case and was dominated by harmonic motion, the underlying behaviour was extracted fitting a series of harmonic sinusoids

$$v_M = \sum_{M=5}^{M} (A_M \sin M\theta + B_M \cos M\theta) + c \tag{4}$$

where v_M is the velocity, θ is the angular position of the reference signal, A_M and B_M are constants. The constants A_M and B_M were obtained using a pseudo-inverse method which yielded a least squares fit for an

over determined set of equations [19]

$$\begin{bmatrix} \sin 1\theta_1 & \sin 2\theta_1 & \dots & \sin M\theta_1 & \cos\theta_1 & \cos 2\theta_1 & \dots & \cos M\theta_1 \\ \sin 1\theta_2 & \sin 2\theta_2 & \dots & & & & & \\ \vdots & & & & & & & \\ \vdots & & & & & & & \\ \sin 1\theta_N & \sin 2\theta_N & \dots & \sin M\theta_N & \cos\theta_N & \cos 2\theta_N & \dots & \cos M\theta_N \end{bmatrix} \begin{bmatrix} A_1 \\ A_2 \\ \vdots \\ A_M \\ B_1 \\ B_2 \\ \vdots \\ B_M \end{bmatrix} = \begin{bmatrix} v_1 \\ v_2 \\ \vdots \\ v_N \end{bmatrix} \tag{5}$$

It was found that $M = 5$ was sufficient in all cases on the basis of minimising the normalised error between the fit and the raw data. However, the analysis technique employed to calculate the time delay between the tube motion and flow reorganisation requires the data to be represented using a single harmonic curve. Hence, Eq. (4) will be the following in practice:

$$v_1 = A_1 \sin\theta_1 + B_1 \cos\theta_1 + c \tag{6}$$

The data used to graphically demonstrate the analysis technique are based on the tests conducted at a free stream flow velocity of $4\,\mathrm{m\,s^{-1}}$ (Figs. 15 and 16). Figs. 15(a) and (b) present the tube motion and flow velocity against angular position, respectively. Also plotted is the respective single harmonic fits and it is observed that the single sinusoid captures the underlying trend in both cases. However, the flow field around the cylinder in a tube array is highly sheared and at some positions it was clear that the flow velocity does not respond linearly to the tube motion. It is therefore important to consider how the quality of the fit was determined. This was determined using a number of criteria. The approach used in this study examined the energy contribution at each harmonic in conjunction with the auto-correlation between the actual data less the first harmonic fit. A good fit was deemed to have been achieved when the energy distribution at the first harmonic was greater than 95%. Below that threshold the fit was deemed to be not of the base line quality. The second criteria also had to be satisfied. This involved examining the auto-correlation of the raw data less the fit of the first harmonic. If the fit was good random noise should be all that remains. Viewing the auto-correlation of this signal determines if the resulting distribution was random or if it contained periodic artefacts.

If the fits from the tube response and the flow velocity are stripped of the DC information, normalised and plotted together (Fig. 16) it is seen that there is a phase difference between the two traces, specifically, the flow velocity lags behind the tube response. Hence, there is a time delay between tube motion and the fluid reorganising which would imply a delay in the resultant force on the cylinder. Using the constants A_1 and B_1 the phase with respect to the reference signal for both fits can be obtained by obtaining the $\tan^{-1} A_1/B_1$. Subtracting the phases between the two traces yields a phase difference, $\Delta\phi$. This was converted into a time

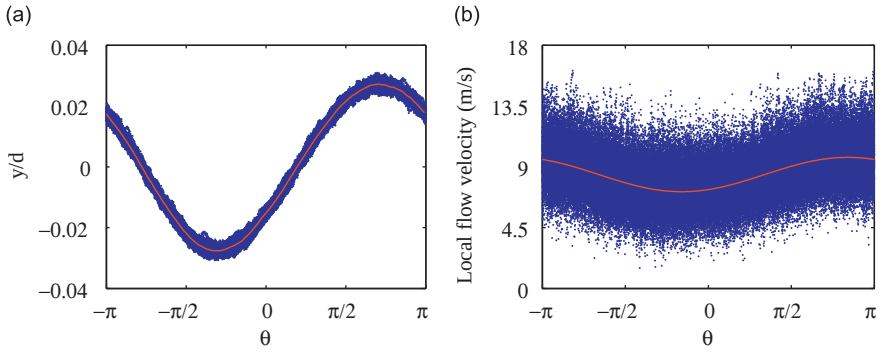

Fig. 15. First harmonic fit of: (a) tube motion and (b) local flow velocity data.

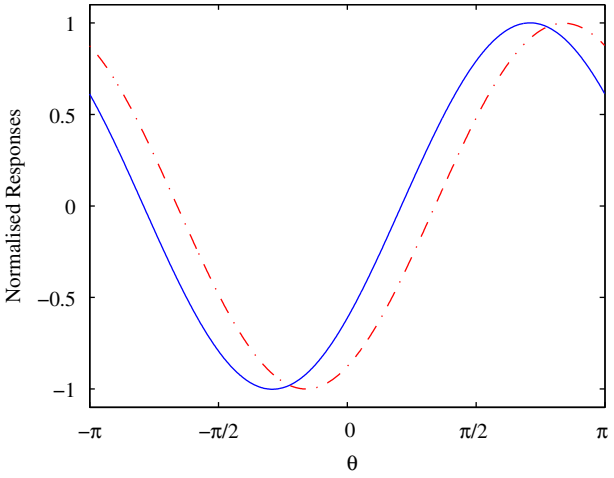

Fig. 16. –, Tube response, and – · –, local flow velocity response, showing a time delay between the two traces.

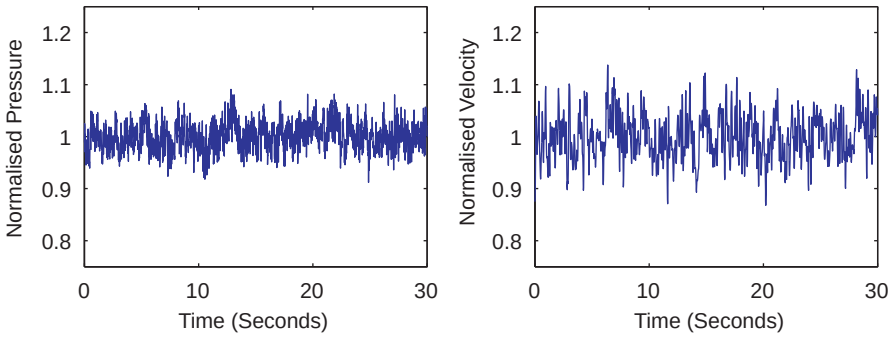

Fig. 17. Normalised pressure and velocity signals at an angular position of $\theta = 80^{\circ}$.

delay, Δt, as the excitation frequency is known:

$$\Delta\phi = \omega\Delta t \tag{7}$$

where $\omega = 2\pi f_n$, f_n is the excitation frequency.

Rearranging and isolating Δt

$$\Delta t = \frac{\Delta\phi}{2\pi f_n} \tag{8}$$

The measured time delay was found to change slightly from test to test with the extent of the deviation from the mean varying with measurement position. On average a deviation of ~10% was observed. This is not surprising given that the time delay has been obtained from a measurement in a flow which is highly sheared and turbulent. It is envisaged that the spread in the measured delay would reduce if the delay was directly measured from the fluid forces on the cylinder. Evidence in support of this argument is shown in Fig. 17 which presents both the normalised pressure and velocity data at $\theta = 80^{\circ}$ when all tubes were rigid. It was observed that the static surface pressure measurements showed smaller deviation from the mean compared to the velocity measurements in the array.

A series of tests were conducted to measure the time delay with and without forced acoustics and each test was repeated five times. Tests were conducted at all positions and flow velocities reported above. It was discussed previously that the measured time delay was found to wander slightly from test to test. The average (of five tests) time delays with and without acoustic resonance are summarised in Table 1. In some instances a change in time delay with forced acoustics occurred but there was an overlap between the individual time

Table 1
Time delay (ms) at a range of positions in the flow field with and without acoustic resonance.

Position	$U = 4\,\mathrm{m\,s^{-1}}$		$U = 7\,\mathrm{m\,s^{-1}}$		$U = 10\,\mathrm{m\,s^{-1}}$	
		AR		AR		AR
15° (*v*-dir)	3.0	0	*3.5*	*3.7*	4.4	2.3
30° (*u*-dir)	5.1	1.4	3.4	5.7	*3.5*	*3.6*
30° (*v*-dir)	6.6	0	*4.9*	*5.4*	5.8	0
90° (*u*-dir)	42.0	45.9	*52.4*	*51.1*	–	–
150° (*u*-dir)	–	–	5.5	9.1	*4.6*	*3.4*
165° (*u*-dir)	9.3	7.9	*7.9*	*8.1*	7.0	6.0
165° (*v*-dir)	10.3	8.1	*8.8*	*9.1*	8.0	6.8

Italic numbers—illustrates the hot-wire positions and velocities where overlap between the individual time delays measured with and without forced acoustics occurs.

delays measured with and without acoustic resonance. These are denoted by the shading in Table 1. In these instances no conclusive outcome as to the influence of acoustic resonance was realised. However, at the other positions a definitive phenomenon emerged: the acoustic resonance modified the time delay. In some instances the time delay was increased; more often the time delay was reduced. The reduced duration of the time delay resulting in a reduction in tube oscillation is in agreement with the model proposed by Price and Paidoussis [10]. Furthermore, the proposition that modification of the time delay shifts the stability threshold is in agreement with the conclusions of Andjelic and Popp [17] which were based on experimental considerations.

It is also apparent from Table 1 that there is variability in the time delays response to acoustic resonance. It is not clear why this is the case. It is possible that there is a flow feature in the tube array but as there is no good physical model for the time delay it is difficult to provide a rigorous conclusion. Further work is required to explore this result but this can only be rigorously examined when the time delay between tube motion and fluid forces is measured.

Assuming that acoustic resonance modifies the time delay, how could this process be justified physically? Granger and Paidoussis [13] formulation of a memory effect (cause of the time delay) refer to vorticity generated on the surface of the cylinder resulting from tube motion. This vorticity is diffused and convected downstream by the mean flow. When the vorticity is convected far enough downstream a new steady state is reached. It was shown that the effect of acoustic resonance on the static fluid forces was negligible (i.e. the vorticity generation process). So, as acoustic resonance was observed to have modified the time delay it must be interfering with the vorticity diffusion–convection process. It was also observed that the acoustic resonance shifted the mean velocity (both increasing and decreasing) at some positions as well as the form of the distribution with reference to the angular position of the tube vibration. This is curious, as at the current tube position the acoustic particle velocity corresponds to a minimum in this region. In this instance it appears that acoustic resonance is causing streaming. It is not unreasonable to suggest that the acoustic streaming may be interfering with the diffusion–convection of vorticity process from the surface of the cylinder suggested by Granger and Paidoussis.

It was discussed above that the effect of acoustic resonance on fluidelastic instability was negligible for a single flexible cylinder in the pitch ratio of 1.58. As a result, the analysis determining the nature of the interaction between acoustic resonance and fluidelastic instability was limited to the pitch ratio of 1.32. However, using the findings from the analysis it will now be discussed as to why acoustic resonance had no effect on the pitch ratio of 1.58. It was reported that jet switching was observed in the pitch ratio of 1.58. It is likely that the jet switching reported to be responsible for the poorly established limit cycle amplitudes also interfered with the convection process (time delay mechanism) destroying any subtle changes in the convection process caused by acoustic resonance. Fig. 4 shows the effect of acoustic resonance on fluidelastic instability in the pitch ratio of 1.32. It was observed that the effect of the forced acoustics on fluidelastic instability was not instantaneous but required time for a new steady state to be reached. It is possible that the jet switching observed in the pitch ratio of 1.58 prevented a cumulative effect. However, this is merely conjectural and further work is required to verify this and the hypothesis that acoustic streaming may be interfering with the diffusion–convection of vorticity process from the surface of the cylinder.

5. Conclusions

It has been shown that acoustic resonance affects fluidelastic instability and this has been quantified. In an attempt to better understand the interaction between fluidelastic instability and acoustic resonance for $P/d = 1.32$ two possibilities are examined based on the framework proposed by Price and Paidoussis [10] to model fluidelastic instability. Acoustic resonance does not change the static fluid force. It has also been shown that at some hot-wire (local flow velocity) positions a definitive change in the time delay between tube motion and the flow field around the cylinder emerged as a result of acoustic resonance. It is also clear that acoustic resonance modifies the mean velocity at some positions in this region where it is thought this results from acoustic streaming. Further work is required to explore the time delay mechanism and hence the effect of acoustic resonance on it.

Acknowledgement

This publication has emanated from research conducted with the financial support of Science Foundation Ireland.

References

[1] S.S. Chen, Instability mechanisms and stability criteria of a group of circular cylinders subjected to cross-flow. Part i: theory, *ASME Journal of Vibrations, Acoustics, Stress, Reliability and Design* 105 (1983) 51–58.
[2] S.J. Price, M.L. Zahn, Fluidelastic behaviour of a normal triangular array subject to cross-flow, *Journal of Fluids and Structures* 5 (1991) 259–278.
[3] C. Meskell, J.A. Fitzpatrick, Investigation of nonlinear behaviour of damping controlled fluidelastic instability in a normal triangular tube array, *Journal of Fluids and Structures* 18 (2003) 573–593.
[4] J. Mahon, C. Meskell, Interaction between acoustic resonance and fluidelastic instability in a normal triangular tube array, *ASME Journal of Pressure Vessel Technology* 131(1) (2009) 011303.
[5] J. Mahon, Interaction Between Acoustic Resonance and Fluidelastic Instability in a Normal Triangular Tube Arrays, PhD Thesis, 2008.
[6] R. Austermann, K. Popp, Stability behaviour of a single flexible cylinder in rigid tube arrays of different geometry subjected to cross-flow, *Journal of Fluids and Structures* 9 (1995) 303–322.
[7] H.C. Yeung, D.S. Weaver, The effect of approach flow direction on the flow-induced vibrations of a triangular tube array, *ASME Journal of Vibration, Acoustics, Stress, and Reliability in Design* 105 (1983) 76–82.
[8] R.D. Blevins, M.M. Bressler, Acoustic resonance in heat exchanger tube bundles—part 1: physical nature of the phenomenon, *ASME Journal of Pressure Vessel Technology* 109 (1987) 275–281.
[9] P.A. Feenstra, D.S. Weaver, F.L. Eisinger, The effects of duct width and baffles on acoustic resonance in a staggered tube array, *Proceedings of the 8th International Conference on Flow-Induced Vibration* Vol. 1 (2004) 459–464.
[10] S.J. Price, M.P. Paidoussis, An improved mathematical model for the stability of cylinder rows subject to cross-flow, *Journal of Sound and Vibration* 97 (4) (1984) 615–640.
[11] A. Simpson, J.W. Fowler, An improved mathematical model for the aerodynamic forces on tandem cylinders in motion with aeroelastic applications, *Journal of Sound and Vibration* 51 (2) (1977) 183–217.
[12] J.A. Fitzpatrick, I.S. Donaldson, W. McKnight, Some observations of the pressure distribution in a tube bank for conditions of self generated acoustic resonance, *International Symposium, Vibration Problems in Industry*, Keswick, UK Paper 3:6, 1978, pp. 1–13.
[13] S. Granger, M. Paidoussis, An improvement to the quasi-steady model with application to cross-flow-induced vibration of tube arrays, *Journal of Fluid Mechanics* 320 (1996) 163–184.
[14] A. Abd-Rabbo, D.S. Weaver, A flow visualisation study of flow development in a staggered tube array, *Journal of Sound and Vibration* 106 (2) (1986) 241–256.
[15] H. Tanaka, S. Takahara, Fluid elastic vibration of tube array in cross flow, *Journal of Sound and Vibration* 77 (1) (1981) 19–37.
[16] S.S. Chen, G.S. Srikantiah, Motion-dependent fluid force coefficients for tubes arrays in crossflow, *ASME Journal of Pressure Vessel Technology* 123 (2001) 429–436.
[17] M. Andjelic, K. Popp, Stability effects in a normal triangular cylinder array, *Journal of Fluids and Structures* 3 (2) (1989) 165–185.
[18] J. Lever, D. Weaver, On the stability of heat exchanger tube bundles. Part i: modified theoretical model. Part ii: numerical results and comparison with experiment, *Journal of Sound and Vibration* 107 (1986) 375–410.
[19] J. Keays, C. Meskell, A study of the behaviour of a single-bladed waste-water pump, *Journal of Process Mechanical Engineering* 220 (2) (2006) 79–87.